Gravitational Waves
Seminaire d'Etudes d'Astrophysique et Techniques Spatiales
Observatoire de Meudon

Bernd MÜLLER-BIERL Fatma SOUFI

February, 1993

Abstract

In this comprehension the theoretical foundations of gravitational waves according to linearized theory of Einsteins equations are outlined. In the following, we present some astrophysical examples of interest in regard to their gravitational wave emission. Moreover, we give a brief introduction in present detector technology and an outlook to future equipment in gravitational waves observatories. For an introduction in the subject the reader might find the book of P.C.W.Davies [1] very instructive. We profited much of the lectures of T.Fliessbach [2], which are mainly based on the book of S. Weinberg [3, chap.10].

We will suppose the reader to be familar at least with the general principles of General Relativity. Beside from that he will find in the appendix a hintful comparison between the basic formulaes displayed in this comprehension and classical electrodynamic wave formalism.

Partial derivatives of an expression x to the coordinate α are expressed $x_{|\alpha}$, spatial components are expressed by bold letters. Latin indices will run from 1 to 3, greek indices from 0 to 3 as usual.

We want to thank Prof. P.Léna, who pleasently contributed to the conceptual design of this comprehension.

Contents

Chapter 1

What are Gravitational Waves ?

1.1 Gravity as a Field

The *equivalence principle* states that gravity *locally* can be simulated by acceleration. Recall that in Special Relativity space-time suffers distortions due to uniform motions. In General Relativity gravitational forces are replaced by the deformation of space-time in a more elaborated way than in Special Relativity.

Within a cube in 3D-space shear, dilatation and rotation can be described by a stress-tensor of $3 \times 3 = 9$ components. In four dimensional space-time deformation is described by the $4 \times 4 = 16$ components of the *energy momentum tensor*, where in General Relativity only 10 components are independent.

Consider as an example a ring of particles in a strong gravitational field (fig. 1.). The ring will suffer *tidal effects* and therefore deform (fig. 2.). This is the relativistic analogon to a solid suffering shear-forces and therefore deforming.

It must be emphasized, that the deformation of the ring according to General Relativity cannot be regarded as a distortion of the ring itself (the particles of the ring even do not need to be coupled), but as deformation of the space-time itself. Tidal effects are no more described by forces, but by the properties of the energy momentum tensor of space-time.

The effect of masses (hence energy according to $E = mc^2$) on space-time is described by the field equations of General Relativity: the *Einstein equations*. They describe the deformation of space-time in terms of the energy momentum tensor.

1.2 Gravitational Waves

Einstein himself already had found that wavelike solutions of his equations exist, where an undulation of space-time propagates with the velocity of light. However, if they could have been transformed away by an acceleration, those distortions only were a mathematical artifice describing undulations in the choice of coordinates.

That there is real physics in the waves first became clear when they were written in terms of the *Riemann curvature tensor*. The Riemann curvature tensor differing from zero describes a real distortion of space-time, not only a change of coordinates.

That gravitational waves exist can be equally argued in the following way: Imagine the Atlas of our days, still insisting on physical fittness, amusing himself in free space by pushing away iron spheres. Due to their gravitational interaction they return, so Atlas has to compensate for their cinetic energy before pushing them away another time [1].

Atlas will find that each time he pushes the masses apart he will have to spend more energy than he gains from the masses comming back. This is explained by the fact that the gravitational field is time retarded due to the finite velocity of light: Each moment where the masses fly appart they suffer the amplified attraction of their constellation at the retardet time corresponding to their actual distance. This works same for the masses comming back, the acceleration now being weakened according to their actual position.

Hence, the energy of the system (Atlas and the iron spheres) decreases. We therefore suppose gravitational waves leaving the system carrying the adequate amount of energy with them.

Conservation of the momentum of the center of mass excludes diplole radiation. We will see that gravitational radiation in its lowest order is *quadrupole radiation*.

Because the waves carry energy, the corresponding particles, the *gravitons*, are "charged" with mass. This is implied by the fact that the field equations, the Einstein equations, are non-linear. In the *weak field approximation* we will neglect the charge of the gravitons by linearizing the Einstein equations.

In the linear aproximation there is no static part of energy, so the waves will travel at the speed of light.

[1] This conspicuous example is more elaborated in the diverting book of J.A.Wheeler, A Journey into Gravity and Spacetime

Chapter 2

Weak Field Approximation

A language being more simple and comprehensible, more free of fault and vague ideas, [...] more dignified to express the inchangeable relations inbetween the natural things [than mathematics] cannot exist.
Joseph FOURIER, Analytical Theorie of Heat (1822)

In comparison to Classical Electrodynamics the interaction between gravity and matter is minute. This is due to the fact, that the *coupling constant for gravity* is about 10^{-40} weaker than that for the electromagnetic force.

Further the gravitational charge, the mass, is *always positive*. It is therefore impossible to construct gravitational dipoles.

We therefore conclude that any observable gravitational radiation is likely to be of very low intensity. This justifies an aproach by linearizing the field equations, as we will do in this chapter.

2.1 General Solution

The Einstein equations

$$R_{\mu\nu} = -\frac{8\pi G}{c^4}\left(T_{\mu\nu} - \frac{T}{2}g_{\mu\nu}\right) \tag{2.1}$$

with the metric tensor $g_{\mu\nu}$, $R_{\mu\nu} = R^{\lambda}{}_{\mu\lambda\nu}$ the Ricci tensor, $R^{\kappa}{}_{\mu\lambda\nu}$ the Riemann curvature tensor, $T_{\mu\nu}$ the energy momentum tensor, $T = T^{\mu}{}_{\mu}$ and the fundamental constants, gravitational coupling constant G and velocity of light c, can be linearized for weak fields

$$g_{\mu\nu} = \eta_{\mu\nu} + h_{\mu\nu}; \quad \text{where } h_{\mu\nu} \ll 1 \tag{2.2}$$

by expressing $R_{\mu\nu}$ in power series of $h_{\mu\nu}$ as

$$R_{\mu\nu} = R_{\mu\nu}{}^{(1)} + R_{\mu\nu}{}^{(2)} + \cdots \tag{2.3}$$

Remark that $R_{\mu\nu}{}^{(0)} = 0$. With

$$R_{\rho\mu\sigma\nu} = \frac{1}{2}\left(g_{\rho\sigma|\mu|\nu} + g_{\mu\nu|\rho|\sigma} - g_{\mu\rho|\nu|\sigma} - g_{\rho\nu|\mu|\sigma}\right) + \mathcal{O}(\Gamma\cdot\Gamma) \tag{2.4}$$

hence

$$R_{\mu\nu}{}^{(1)} = R^{\rho}{}_{\mu\nu\rho}{}^{(1)} = \frac{1}{2}\left(\Box h_{\mu\nu} + h^{\rho}{}_{\rho|\mu|\nu} - h^{\rho}{}_{\mu|\rho|\nu} - h^{\rho}{}_{\nu|\rho|\mu}\right) \tag{2.5}$$

we obtain in first order of h

$$\Box h_{\mu\nu} + h^{\rho}{}_{\rho|\mu|\nu} - h^{\rho}{}_{\mu|\rho|\nu} - h^{\rho}{}_{\nu|\rho|\mu} = -\frac{16\pi G}{c^4}\left(T_{\mu\nu} - \frac{T}{2}\eta_{\mu\nu}\right) \tag{2.6}$$

We now consider the invariance of the field equations 2.6 according to coordinate transformations:

$$x^{\mu} \longrightarrow x'^{\mu} = x^{\mu} + \epsilon^{\mu}(x) \tag{2.7}$$

In our weak field approximation we must restrict on small deviations from Minkowskian coordinates $\partial\epsilon/\partial x = \mathcal{O}(h)$. In the new metric tensor

$$g'_{\mu\nu} = \frac{\partial x'_{\mu}}{\partial x_{\lambda}}\frac{\partial x'_{\nu}}{\partial x_{\kappa}} g_{\lambda\kappa} = \eta_{\mu\nu} + h'_{\mu\nu} \tag{2.8}$$

we insert

$$\frac{\partial x'_{\mu}}{\partial x_{\lambda}} = \delta^{\lambda}_{\mu} + \frac{\partial \epsilon_{\mu}}{\partial x_{\lambda}} \tag{2.9}$$

and $g_{\lambda\kappa} = \eta_{\lambda\kappa} + h_{\lambda\kappa}$. This leads to the gauge transformation of the potentials $g_{\mu\nu}$

$$h_{\mu\nu} \longrightarrow h'_{\mu\nu} = h_{\mu\nu} + \epsilon_{\mu|\nu} + \epsilon_{\nu|\mu} \tag{2.10}$$

The possibility of these transformations allows us to demand conditions on the potentials $h_{\mu\nu}$. We demand the 4 gauge conditions

$$2h^{\mu}{}_{\nu|\mu} = h^{\mu}{}_{\mu|\nu} \tag{2.11}$$

These conditions determine the 4 gauge fields $\epsilon_{\mu}(x)$ With 2.11 we obtain from 2.6 the *decoupled linearized field equations*

$$\Box h_{\mu\nu} = -\frac{16\pi G}{c^4}\left(T_{\mu\nu} - \frac{T}{2}\eta_{\mu\nu}\right) \tag{2.12}$$

With the abbrevation $S_{\mu\nu} = T_{\mu\nu} - \eta_{\mu\nu}T/2$ we recognize 2.12 being of the same structure as the decoupled field equations of electrodynamics (see appendix). We can write down the general solution in terms of the retarded potentials

$$h_{\mu\nu}(\mathbf{x},t) = -\frac{4G}{c^4}\int d^3x' \frac{S_{\mu\nu}(\mathbf{x}', t - |\mathbf{x}-\mathbf{x}'|/c)}{|\mathbf{x}-\mathbf{x}'|} \tag{2.13}$$

The retarded time argument in 2.13 significates that changes in the source term propagate with the velocity of light. The advanced potentials formally also would be a solution of 2.12, but they do not obey causality.

The gauge 2.11 implicates the choice of coordinates. The significance of the thereby determined coordinates becomes clear from the physical distances $ds^2 = (\eta_{\mu\nu} + h_{\mu\nu})dx^{\mu}dx^{\nu}$ with $h_{\mu\nu}$ calculated from 2.13. Analogeous to electrodynamics, the physics is independent from the gauge, that is independent from the selected coordinates.

2.2 Plane Waves

We now are interested in plane gravitation waves. The linearized field equations hold only for weak fields, that is

$$|\, h_{\mu\nu} \,| \ll 1, \quad \text{and} \quad |\, \epsilon_{\mu} \,| \ll 1 \tag{2.14}$$

for we will in the following restrict on the dominant order in h and ϵ. Hence the change between co- and contravariant components can be done with $\eta_{\mu\nu}$ and the covariant derivative becomes the partial derivative.

The freedom in the choice of 4 functions ϵ in 2.7 corresponds to the freedom in the choice of 4 gauge conditions. The 4 gauge conditions 2.11

$$2h^{\mu}{}_{\nu|\mu} = h^{\mu}{}_{\mu|\nu} \tag{2.15}$$

are choosen that the linearized field equations 2.6 decouple and therefore lead to 2.12.

Because of $h_{\mu\nu} = h_{\nu\mu}$, there are only 6 components independent. For the free equations

$$\Box h_{\mu\nu} = 0 \tag{2.16}$$

another 4 gauge transformations are possible with functions ϵ, which obey the wave equation $\Box\epsilon^{\mu} = 0$. This finally reduces the number of independant components to 2. We show in the following the reduction from 10 to 2 fields explicitally. First we write down the solution of 2.16 in plane waves:

$$h_{\mu\nu} = e_{\mu\nu}\exp(-ik_{\lambda}x^{\lambda}) + c. \tag{2.17}$$

therefore

$$\eta^{\lambda\kappa}k_{\lambda}k_{\kappa} = k^{\lambda}k_{\kappa} \quad \text{or} \quad k_0^2 = \frac{\omega^2}{c^2} = k^2 \tag{2.18}$$

where $k = |\,\mathbf{k}\,|$. The amplitudes $e_{\mu\nu}$ are called *polarization tensor*. The gauge condition 2.11 produces therefore

$$2k_{\mu}\eta^{\rho\sigma}e_{\rho\nu} = k_{\nu}\eta^{\rho\sigma}e_{\rho\mu} \tag{2.19}$$

Like the $h_{\mu\nu}$ the polarization tensor has to be symetric,

$$e_{\mu\nu} = e_{\nu\mu} \tag{2.20}$$

For simplicity we consider a wave in x^3-direction:

$$h_{\mu\nu} = e_{\mu\nu}\exp(-ikx^3 - ict) + c. \tag{2.21}$$

hence

$$k_1 = k_2 = 0, \quad k_0 = -k_3 = k = \frac{\omega}{c} \tag{2.22}$$

Hence the conditions 2.19 are in extensio

$$\begin{aligned} e_{00} + e_{30} &= (e_{00} - e_{11} - e_{22} - e_{33})/2 && (2.23)\\ e_{01} + e_{31} &= 0 && (2.24)\\ e_{02} + e_{32} &= 0 && (2.25)\\ e_{03} + e_{33} &= -(e_{00} - e_{11} - e_{22} - e_{33})/2 && (2.26) \end{aligned}$$

Considering the symetrie $e_{\mu\nu} = e_{\nu\mu}$ and these 4 conditions the polarization tensor can be determined by 6 components:

$$\text{Independent components}: e_{00}, e_{11}, e_{33}, e_{12}, e_{13}, \text{ and } e_{23} \tag{2.27}$$

These components determine the other components:

$$e_{01} = -e_{31},\ e_{02} = -e_{32},\ e_{03} = -\frac{e_{33} + e_{00}}{2},\ e_{22} = -e_{11} \tag{2.28}$$

There are gauge transformations possible for the solution of the free equations 2.16. Those are transformations 2.7 with functions $\epsilon^\mu(x)$, which are solutions of the free wave equation 2.16:

$$\epsilon^\mu(x) = \delta^\mu \exp(-ik_\lambda x^\lambda) + c. \tag{2.29}$$

From a solution of the wave equations $h_{\mu\nu}$ we obtain another solution corresponding 2.10. It rests to be shown that the transformation is in accord with the gauge conditions 2.11. Therefore the aditional terms in the gauge condition must vanish, hence

$$2\left(\epsilon^\mu{}_{\nu} + \epsilon^\nu{}_{\mu}\right)_{|\mu} = \left(\epsilon^\mu{}_{\mu} + \epsilon^\mu{}_{\mu}\right)_{|\nu} \tag{2.30}$$

This is satisfied because of $\Box\epsilon_\nu(x) = 0$.
We insert 2.17 and 2.29 into 2.10. Therefore we obtain the amplitudes $e'_{\mu\nu}$ of $h'_{\mu\nu}$:

$$e'_{\mu\nu} = e_{\mu\nu} + ik_\mu\delta_\nu + ik_\nu\delta_\mu \tag{2.31}$$

With 2.22 we obtain for the independent 6 amplitudes:

$$\begin{aligned} e'_{11} &= e_{11} && (2.32)\\ e'_{12} &= e_{12} && (2.33)\\ e'_{13} &= e_{13} - ik\delta_1 && (2.34)\\ e'_{22} &= e_{22} - ik\delta_2 && (2.35)\\ e'_{33} &= e_{33} - 2ik\delta_3 && (2.36)\\ e'_{00} &= e_{00} + 2ik\delta_0 && (2.37) \end{aligned}$$

With a gauge transformation 2.10 with 2.29 we can replace the $e_{\mu\nu}$ by $e'_{\mu\nu}$. For the $e'_{\mu\nu}$ we eliminate by properly selecting the δ_μ the amplitudes e'_{13}, e'_{23}, e'_{33} and e'_{00}. Only e'_{12} and e'_{11} rest. Hence we have the general form of a plane wave in x^3-direction:

$$(h_{\mu\nu}) = \begin{pmatrix} 0 & 0 & 0 & 0\\ 0 & e_{11} & e_{12} & 0\\ 0 & e_{12} & -e_{11} & 0\\ 0 & 0 & 0 & 0 \end{pmatrix} \exp(ikx^3 - ict) + c. \tag{2.38}$$

This wave has two possible linear polarizations, significated by $e_{12} = 0$ respectively $e_{11} = 0$.
We now consider the spin of the wave. Because we have a near Minkowskian metric, we describe a rotation as Lorentztransformation. A rotation around the x^3-axis with angle θ is described by the matrix

$$(\bar{\Lambda}^\mu_\nu) = \begin{pmatrix} 1 & 0 & 0 & 0\\ 0 & \cos\phi & \sin\phi & 0\\ 0 & -\sin\phi & \cos\phi & 0\\ 0 & 0 & 0 & 1 \end{pmatrix} \tag{2.39}$$

The polarization tensor is transformed according to

$$e'_{\mu\nu} = \bar{\Lambda}^\rho_\mu \bar{\Lambda}^\sigma_\nu e_{\rho\sigma} \tag{2.40}$$

Equivalent to the 6 amplitudes in 2.27 are

$$e_\pm = e_{11} \pm ie_{12},\ f_\pm = e_{13} \pm ie_{23},\ e_{00},\ e_{33} \tag{2.41}$$

With the transformation law 2.40,2.39 for these amplitudes results:

$$\begin{aligned} e'_\pm &= \exp(\pm 2i\phi)e_\pm && (2.42)\\ f'_\pm &= \exp(\pm i\phi)f_\pm,\ e'_{33} = e_{33},\ e'_{00} = e_{00} && (2.43) \end{aligned}$$

The law of transformation of a plane wave

$$\Psi' = \exp(ih\phi)\Psi \tag{2.44}$$

under rotation around the wave vector k is called spin h. In a quantisized theory $h_{\mu\nu}$ becomes the wavefunction of the gravitons. The values for $h = 0, \pm 1, \pm 2$ in 2.43 and 2.43 show that the gravitons are particles with spin 2.
As we have seen above, the contributions with e_{00}, e_{33}, e_{11} and e_{23} can allways be eliminated by properly selecting coordinates. Therefore these contibutions have no physical significance. Corresponding 2.41 and 2.43 these are the spins $h = 0$ and $h = \pm 1$. On the contrary $h = \pm 2$ significates a physical property of the wave, hence a state of the graviton.

2.3 Particles in the Field of the Wave

From equation 2.2 follows that a line element in the weak field approximation is given by

$$ds^2 = (\eta_{\mu\nu} + h_{\mu\nu})dx^\mu dx^\nu \tag{2.45}$$

The trajectories of particles $x^\sigma(\tau)$ in a gravitational field are given by the equation of geodesics

$$\frac{d^2x^\sigma}{d\tau^2} = -\Gamma^\sigma_{\mu\nu}\frac{dx^\mu}{d\tau}\frac{dx^\nu}{d\tau} \tag{2.46}$$

with the Christoffel symbols $\Gamma^{\sigma}_{\mu\nu}$. The equations 2.38, 2.45 and 2.46 define the scope of this section. From

$$\Gamma^{\sigma}_{\mu\nu} = \frac{\eta^{\sigma\lambda}}{2}\left(h_{\nu\lambda|\mu} + h_{\mu\lambda|\nu} - h_{\mu\nu|\lambda}\right) \tag{2.47}$$

follows for the field 2.38

$$\Gamma^{\sigma}_{00} = -\frac{1}{2}\left(h_{0\sigma|0} + h_{0\sigma|0} - h_{00|\sigma}\right) = 0 \tag{2.48}$$

We chose the initial conditions $dx^{i}/d\tau = 0$ at time $\tau = 0$. There we have

$$\left(\frac{dx^{\sigma}}{d\tau}\right)_{\tau=0} = (c,0) \overset{2.46,2.48}{\rightarrow} \left(\frac{d^2x^{\sigma}}{d\tau^2}\right)_{\tau=0} = 0 \tag{2.49}$$

For the acceleration in the selected coordinates vanishes, the velocity rests constant. We have hence as solution of 2.46

$$\frac{dx^{i}}{d\tau} = 0, \quad \text{hence } x^{i}(\tau) = c. \tag{2.50}$$

We have described the particles in the field of the wave by constant spatial coordinates. This does not mean that the particles are at rest. Rather the relative distances change due to the time dependance of the metric tensor 2.45.

We especially consider particles ordered on a ring in the x^1-x^2-plane, see figure 1. From 2.38 and 2.45 follows for the physical distance between particles

$$dl^2 = [\delta_{mn} - h_{mn}(t)] \overset{!}{=} dx^m dx^n (m,n = 1,2) \tag{2.51}$$

where

$$(h_{mn}(t)) = \begin{pmatrix} e_{11} & e_{12} \\ e_{12} & -e_{11} \end{pmatrix} \exp(-i\omega t) + c. \tag{2.52}$$

For the metric coefficients do not depend on $x = x^1$ and $y = x^2$ we can apply 2.51 directly to finite values x^m of the particles in figure 1. , hence for

$$x^1 = R\cos(\phi), \quad x^2 = R\sin(\phi) \tag{2.53}$$

From 2.51 to 2.53 we obtain for the physical distances R_h of the particles from the center:

$$R_h^2 = x^2 + y^2 = R^2 \cdot \begin{cases} [1 - 2h\cos(2\phi)\cos(\omega t)] \text{ case} & (e_{11} = h, e_{12} = 0) \\ [1 - 2h\sin(2\phi)\cos(\omega t)] \text{ case} & (e_{12} = h, e_{11} = 0) \end{cases} \tag{2.54}$$

There we have distinguished the two possible linear polarizations. The amplitude of the wave is denoted h.

The physical deviations $x = R_h\cos(\phi)$ and $y = R_h\sin(\phi)$ are shown in figure 2. The 2 independant directions of polarization include an angle $\pi/4$. Circular or eliptic polarized waves can be constructed, where the axes of the deformed ellipsis are turning in time. The linear combinations $e_{\pm}$ for circular polarization are given in 2.41.

The deviations shown in figure 2. significate an oscillating quadrupole moment of the mass distribution. In contrary a mass distribution with an oscillating quadrupole moment will emmit gravitational waves. To examine the power of the radiation we need the energy momentum tensor of the gravitational wave.

2.4 Energy and Momentum of the Wave

In electrodynamics the density of energy and momentum is of power 2 in the fields, hence of power 2 in the derivatives $A_{\alpha|\beta}$ of the potentials. In analogie we estimate fields of power 2 in the $h_{\mu\nu|\lambda}$. For a wave with amplitude h is $h_{\mu\nu|\lambda} \sim k_\lambda h$. Because these terms are part of $G_{\mu\nu}$ on the left side of the field equations, they get a factor $c^4/8\pi G$ when writing them to the energie momentum tensor of the source terms. We therefore estimate the energie momentum tensor of a gravitational wave to be

$$t_{\mu\nu} \sim \frac{c^4}{8\pi G} k_\mu k_\nu h^2 \tag{2.55}$$

In this section we calculate the exact expression for $t_{\mu\nu}$. We start again from a weak field

$$g_{\mu\nu} = \eta_{\mu\nu} + h_{\mu\nu}; \qquad (h_{\mu\nu} \ll 1) \tag{2.56}$$

and the plane wave

$$h_{\mu\nu} = e_{\mu\nu}\exp(-ik_\lambda x^\lambda) + c. \tag{2.57}$$

This wave is solution of the wave equations in first order in h, hence

$$R^{(1)}_{\mu\nu} = 0 \tag{2.58}$$

To obtain the energy momentum tensor of the wave we must consider the second order terms in 2.3. We suppose near Minkowskian coordinates, therefore introducing the d'Alembert operator

$$\partial^\mu\partial_\mu = \Box + \mathcal{O}(h) \tag{2.59}$$

The scalar of curvature in first order in h is

$$R^{(1)} = \eta^{\lambda\rho} R_{\lambda\rho}{}^{(1)} \tag{2.60}$$

We comprehend the terms in second order in h to a tensor $t_{\mu\nu}$,

$$R_{\mu\nu}{}^{(2)} - \left(\frac{Rg_{\mu\nu}}{2}\right)^{(2)} = \frac{c^4}{8\pi G}\, t_{\mu\nu} \tag{2.61}$$

Hence the field equations in second order in h are:

$$R_{\mu\nu}{}^{(1)} - \frac{R^{(1)}}{2}\eta_{\mu\nu} = -\frac{8\pi G}{c^4}(T_{\mu\nu} + t_{\mu\nu}) \tag{2.62}$$

This equation is of the form of a wave equation linear in the $h_{\mu\nu}$ (compare 2.5) with source terms

$$\tau_{\mu\nu} = T_{\mu\nu} + t_{\mu\nu} \tag{2.63}$$

Thereby $\tau_{\mu\nu}$ is the energy momentum tensor. Because $T_{\mu\nu}$ contains the non-gravitational terms, $t_{\mu\nu}$ is the energy momentum tensor of the gravitational field:

$$t_{\mu\nu} = \frac{c^4}{8\pi G}\left[R_{\mu\nu}{}^{(2)} - \left(\frac{Rg_{\mu\nu}}{2}\right)^{(2)}\right] \tag{2.64}$$

We evaluate it with $R = g^{\rho\sigma}R_{\rho\sigma}$ and 2.58:

$$t_{\mu\nu} = \frac{c^4}{16\pi G}\left[2R_{\mu\nu}{}^{(2)} - \eta_{\mu\nu}\eta^{\rho\sigma}R_{\sigma\rho}{}^{(2)} + \eta_{\mu\nu}h^{\rho\sigma}R_{\sigma\rho}{}^{(1)} - h_{\mu\nu}\eta^{\rho\sigma}R_{\rho\sigma}{}^{(1)}\right]$$
$$= \frac{c^4}{16\pi G}\left[2R_{\mu\nu}{}^{(2)} - \eta_{\mu\nu}\eta^{\rho\sigma}R_{\sigma\rho}{}^{(2)}\right] \quad (2.65)$$

The Ricci tensor

$$R_{\mu\kappa}{}^{(2)} = \left(g^{\lambda\nu}R_{\lambda\mu\nu\kappa}\right)^{(2)} = \eta^{\lambda\nu}R_{\lambda\mu\nu\kappa}{}^{(2)} - h^{\lambda\nu}R_{\lambda\mu\nu\kappa}{}^{(1)} \quad (2.66)$$

is defined by the Riemann curvature tensor

$$R_{\lambda\mu\nu\kappa} = \frac{1}{2}\left(\frac{\partial^2 g_{\lambda\nu}}{\partial x^\mu \partial x^\kappa} + \frac{\partial^2 g_{\mu\kappa}}{\partial x^\lambda \partial x^\nu} - \frac{\partial^2 g_{\mu\nu}}{\partial x^\lambda \partial x^\kappa} - \frac{\partial^2 g_{\lambda\kappa}}{\partial x^\mu \partial x^\nu}\right)$$
$$+ g_{\eta\sigma}\left(\Gamma^\eta_{\nu\lambda}\Gamma^\sigma_{\mu\kappa} - \Gamma^\eta_{\kappa\lambda}\Gamma^\sigma_{\mu\nu}\right) \quad (2.67)$$

The Christoffel symbols are to be calculated in first order:

$$\Gamma^\sigma_{\mu\nu} = \frac{1}{2}\left[h^\sigma{}_{\mu|\nu} + h^\sigma{}_{\nu|\mu} - \frac{\partial h^{\mu\nu}}{\partial x_\sigma}\right] \quad (2.68)$$

hence for 2.66

$$R_{\mu\kappa}{}^{(2)} = -\frac{h_{\lambda\nu}}{2}\left(\frac{\partial^2 h_{\lambda\nu}}{\partial x^\mu \partial x^\kappa} + \frac{\partial^2 h_{\mu\kappa}}{\partial x^\lambda \partial x^\nu} - \frac{\partial^2 h_{\mu\nu}}{\partial x^\lambda \partial x^\kappa} - \frac{\partial^2 h_{\lambda\kappa}}{\partial x^\mu \partial x^\nu}\right)$$
$$+\frac{1}{4}\left[h^\nu{}_{\sigma|\nu} + h^\nu{}_{\sigma|\nu} - h^\nu{}_{\nu|\sigma}\right]\times\left[h^\sigma{}_{\mu|\kappa} + h^\sigma{}_{\kappa|\mu} - \frac{\partial h^{\mu\kappa}}{\partial x_\sigma}\right]$$
$$-\frac{1}{4}\left[h_{\sigma\kappa|\lambda} + h_{\sigma\lambda|\kappa} - h_{\lambda\kappa|\sigma}\right]\times\left[\frac{\partial h^\sigma{}_\mu}{\partial x_\lambda} + h^{\sigma\lambda}{}_{|\mu} - \frac{\partial h^\lambda{}_\mu}{\partial x_\sigma}\right] \quad (2.69)$$

For the gauge condition 2.11 the second line of 2.67 disappears. The other terms are of power 2 in h and look like

$$\left[e_{..}\exp(-ik_\lambda x^\lambda) + c.\right]\left[e_{..}\exp(-ik_\lambda x^\lambda) + c.\right] \quad (2.70)$$

There we have oscillating terms with $\exp(\pm ik_\lambda x^\lambda)$, but also coordinate independent terms. The oscillating terms vanish in the temporal mean, hence

$$\left\langle\left[e_{..}\exp(-ik_\lambda x^\lambda) + c.\right]\left[e_{..}\exp(-ik_\lambda x^\lambda) + c.\right]\right\rangle = 2\Re\left\{e_{..}{}^*\right\} \quad (2.71)$$

where $\langle\ldots\rangle$ denotes the temporal mean and $\Re$ the real part. For the wave 2.57 the derivatives correspond to

$$\frac{\partial}{\partial x^\lambda}(\ldots) = -ik_\lambda(\ldots) \quad (2.72)$$

Therefore and with 2.71 we obtain

$$\langle R_{\mu\kappa}{}^{(2)}\rangle = \Re\left\{e^{\lambda\nu *}\left[k_\mu k_\kappa e_{\lambda\nu} + k_\lambda k_\nu e_{\mu\kappa} - k_\lambda k_\kappa e_{\mu\nu} - k_\mu k_\nu e_{\lambda\kappa}\right]\right\}$$
$$- \Re\left\{\frac{1}{2}\left[k_\lambda e_{\sigma\kappa} + k_\lambda e_{\sigma\lambda} - k_\sigma e_{\lambda\kappa}\right]^*\left[k^\lambda e^\sigma{}_\mu + k_\mu e^{\sigma\lambda} - k^\sigma e^\lambda_\mu\right]\right\} \quad (2.73)$$

This can be simplified by 2.19, we have

$$e^{\lambda\nu *}k_\kappa k_\lambda e_{\mu\nu} = \frac{1}{2}k^\nu(e^\lambda{}_\lambda)^* K_\kappa e_{\mu\nu} = \frac{1}{4}k_\mu k_\kappa \mid e^\lambda{}_\lambda \mid^2 \quad (2.74)$$

With regard to $k^\lambda k_\lambda = 0$ 2.73 becomes

$$\langle R_{\mu\kappa}{}^{(2)}\rangle = k_\mu k_\kappa\left[e^{\lambda\kappa *}e_{\lambda\kappa} - \frac{1}{2}\mid e^\lambda{}_\lambda \mid^2\right] \quad (2.75)$$

Hence the energy momentum tensor for the wave 2.65 is

$$t_{\mu\nu} = \frac{c^4}{16\pi G}k_\mu k_\kappa\left[e^{\lambda\kappa *}e_{\lambda\kappa} - \frac{1}{2}\mid e^\lambda{}_\lambda \mid^2\right] \quad (2.76)$$

This can be understood as follows: The momentum flux ($\propto t_{0\nu}$) of the wave must be proportional to the wave vector k_ν, therefore results $t_{0\nu} \propto k_\nu$ and $t_{\mu\nu} \propto k_\mu{}_\nu$. Together with the above established factor (2.55) this results in

$$t_{\mu\nu} = \frac{c^4}{16\pi G}k_\mu k_\nu \cdot \text{ scalar} \quad (2.77)$$

The scalar must be in power 2 in the amplitudes $e_{\lambda\kappa}$. Therefore the two occurrent combinations appear.

As for every energy momentum tensor, t_{00} is the density of energy and t_{0i}/c the density of momentum of the field. Especially the energy flux Φ in x^3-direction is

$$\Phi = ct_{03} \quad (2.78)$$

This is the energy per unit time and surface element: an energy flux density.

2.5 Quadrupole Radiation

Like an oscillating electric charge emitts electromagnetic radiation, an oscillating mass distribution may emit gravitational radiation. The aim of this section is to calculate the emitted power P.

Apart from factors of magnitude 1 we can estimate the result in analogie to electrodynamics. For dipole radiation holds [1]

$$P = \frac{\omega^4}{3c^2}p^2 \quad (2.79)$$

with the oscillator frequency ω and the dipole moment $p \sim ql$; whereas q and l hold for the charge and the characteristic amplitude. For the electric quadrupole radiation the factor $\exp(ikr)$ in the retarded potential has to be developped one power in $kr = \omega r/c$ further. The radiation power therefore becomes

[1] See textbooks on electrodynamics

$$P = \frac{\omega^6}{c^5} Q_e^2 \tag{2.80}$$

For an oscillating mass distribution the dipole moment vanishes according to the conservation of total momentum. The characteristic quantity of the mass quadrupole moment $Q \sim Ml^2$ leads with q^2 corresponding to GM^2 to

$$P = \frac{\omega^6}{c^5} G Q^2 \tag{2.81}$$

We determine in the following an exact expression for P and its angular distribution $dP/d\omega$. We disposite the calculation in the following order:

1. Asymptotic fields from the source terms $T_{\mu\nu}$
2. Reduction to the spatial components T_{ij}
3. Approximation of long waves

Fields from the $T_{\mu\nu}$

We start from a spatial limited periodic mass distribution

$$T_{\mu\nu}(\mathbf{r},t) = T_{\mu\nu}(\mathbf{r}) \exp(-\imath\omega t) + c. = \begin{cases} \neq 0 & (r \leq r_0) \\ = 0 & (r > r_0) \end{cases} \tag{2.82}$$

The retarded potentials are given by 2.13

$$h_{\mu\nu}(\mathbf{r},t) = -\frac{4G}{c^4} \exp(-\imath\omega t) \int d^3r' S_{\mu\nu}(\mathbf{r}') \frac{\exp(ik \mid \mathbf{r} - \mathbf{r}' \mid)}{\mid \mathbf{r} - \mathbf{r}' \mid} + c. \tag{2.83}$$

with $S_{\mu\nu} = T_{\mu\nu} - \eta_{\mu\nu}/2$. With the assumption

$$r_0 \ll \lambda \ll r \tag{2.84}$$

we calculate the power of the radiation. We develop 2.83 for far distances ($r \gg r_0$):

$$\begin{aligned} h_{\mu\nu}(\mathbf{r},t) &= -\frac{4G}{c^4} \frac{\exp(ikr - i\omega t)}{r} \int d^3r' S_{\mu\nu}(\mathbf{r}') \exp(-\imath\mathbf{k}\mathbf{r}') + c. \\ &= e_{\mu\nu}(\mathbf{r},t) \exp(-ik_\lambda x^\lambda) + c. \end{aligned} \tag{2.85}$$

with

$$e_{\mu\nu}(\mathbf{r},t) = -\frac{4G}{c^4 r} \int d^3r' S_{\mu\nu}(\mathbf{r}') \exp(-\imath\mathbf{k}\mathbf{r}') + c. \tag{2.86}$$

and

$$(k^\lambda) = \left(\frac{\omega}{c}, k\right), \quad \mathbf{k} = k\frac{\mathbf{r}}{r} \tag{2.87}$$

Notice that the amplitude $e_{\mu\nu}(\mathbf{r},t)$ is proportional to $1/r$ and does depend on the direction of $\mathbf{r}$. Moreover, it's a function of $\omega = ck$. It is mainly determined by

$$S_{\mu\nu}(\mathbf{k}) = T_{\mu\nu}(\mathbf{k}) - \eta_{\mu\nu}\frac{T(\mathbf{k})}{2} \tag{2.88}$$

hence the Fourier transformed $T_{\mu\nu}(\mathbf{k})$ of $T_{\mu\nu}(\mathbf{r})$.

The energy flux dP passing by the surface element $r^2 d\Omega$ is given by the energy momentum tensor of the gravitational $t_{\mu\nu}$ field:

$$dP = ct_{0i}df^i = ct_{0i}\frac{x^i}{r} r^2 d\Omega \tag{2.89}$$

We insert the t^{0i} from 2.76 with the $e_{\mu\nu}$ from 2.86. Here we have to make an annotation: In the section 2.4 the amplitudes $e_{\mu\nu}$ were constants, whereas according to 2.86 $e_{\mu\nu}(\mathbf{r},t) \propto 1/r$ holds. The energy momentum tensor 2.65, 2.69 as function of the potentials $h_{\mu\nu}$ contains partial derivatives which produce a factor k_μ in the case of constant amplitudes. In the case $e_{\mu\nu}(\mathbf{r},t) \propto 1/r$ those derivatives additionally produce terms with a factor $1/r$ instead of $k_\mu \sim \lambda^{-1}$. While assuming the point of view far enough, $r \gg \lambda$, those terms can be neglected.

We now evaluate 2.89 with 2.76, 2.86 and 2.88:

$$\frac{dP}{d\Omega} = \frac{G\omega^2}{\pi c^5}\left[T^{\mu\nu}(\mathbf{k})^* T^{\mu\nu}(\mathbf{k}) - \frac{1}{2} \mid T^{\mu\nu}(\mathbf{k}) \mid^2\right] \tag{2.90}$$

There we have expressed the power of the radiation by the Fourier transformed $T_{\mu\nu}(\mathbf{k})$ of the source distribution.

Reduction on the spatial components

Using the continuity equation we express $dP/d\Omega$ by the spatial components T^{ij}.

For in the weak field approximation covariant derivations become partial, the continuity equation is

$$T^{\mu\nu}{}_{|\nu} = 0 \tag{2.91}$$

The distribution of the source 2.82 can be written

$$\begin{aligned} T^{\mu\nu}(\mathbf{r},t) &= \frac{1}{2\pi}\int d^3k T^{\mu\nu}(\mathbf{k}) \exp(i\mathbf{k}\mathbf{r} - i\omega t) + c. \\ &= \frac{1}{2\pi}\int d^3k T^{\mu\nu}(\mathbf{k}) \exp(-ik_\lambda x^\lambda) + c. \end{aligned} \tag{2.92}$$

The continuity equation therefore is

$$k_\nu T^{\mu\nu} = 0 \tag{2.93}$$

Hence we find

$$T^{i0} = T^{0i} = \hat{k}_j T^{ij}, \quad T^{00} = \hat{k}_i \hat{k}_j T^{ij} \tag{2.94}$$

with $\hat{k}_i = k_i/k_0$. With this we can eliminate all spatial components in 2.90. We obtain

$$
\begin{aligned}
T^{\mu\nu*}T_{\mu\nu} &= \eta_{\mu\rho}\eta_{\nu\sigma}T^{\mu\nu*}T^{\rho\sigma} \\
&= T^{00*}T^{00} - 2\sum_{i} T^{0i*}T^{0i} + \sum_{i,j} T^{ij*}T^{ij} \\
&= \left(\hat{k}_i\hat{k}_j\hat{k}_l\hat{k}_m - 2\hat{k}_j\hat{k}_m\delta_{il} + \delta_{il}\delta_{jm}\right) T^{ij*}T_{lm} \qquad (2.95) \\
T^{\lambda}{}_{\lambda} &= \eta_{\lambda\rho}T^{\rho\lambda} = T^{00} - \sum_{i} T^{ii} \\
&= \left(\hat{k}_i\hat{k}_j - \delta_{ij}\right) T^{ij*}T^{ij} \qquad (2.96)
\end{aligned}
$$

We inset these expressions in 2.90:

$$
\frac{dp}{d\Omega} = \frac{G\omega^2}{\pi c^5}\Lambda_{ij,lm}T^{ij*}(\mathbf{k})T^{lm}(\mathbf{k}) \qquad (2.97)
$$

where

$$
\begin{aligned}
\Lambda_{ij,lm}(\theta,\phi) = \delta_{il}\delta_{jm} &- \frac{1}{2}\delta_{ij}\delta_{lm} - 2\delta_{il}\hat{k}_j\hat{k}_m + \frac{1}{2}\delta_{ij}\hat{k}_l\hat{k}_m \\
&+ \frac{1}{2}\delta_{lm}\hat{k}_i\hat{k}_j + \frac{1}{2}\hat{k}_i\hat{k}_j\hat{k}_l\hat{k}_m \qquad (2.98)
\end{aligned}
$$

is a function of of the angles θ and ϕ of the vector $\hat{\mathbf{k}} = \mathbf{k}/k$.

Approximation of long waves

We now suppose that the velocities in the mass distribution $v \sim \omega r_0$ are non-relativistic, hence

$$
v \ll c \quad or \quad \lambda \gg r_0 \qquad (2.99)
$$

So we can use the long wave approximation

$$
\begin{aligned}
T^{ij}(\mathbf{k}) &= \int d^3r T^{ij}(\mathbf{r})\exp(-i\mathbf{kr}) = \int d^3r T^{ij}(\mathbf{r})(1 - i\mathbf{kr} + \ldots) \\
&\simeq \int d^3r T^{ij}(\mathbf{r}) \equiv -\frac{\omega^2}{2}Q^{ij} \qquad (2.100)
\end{aligned}
$$

From the continuity equation 2.91 we obtain

$$
T^{ij}{}_{|i|j}(\mathbf{r},t) = \frac{\omega^2}{c^2}T^{00}(\mathbf{r}) \qquad (2.101)
$$

So we can transform 2.100

$$
2\int d^3r T^{ij}(\mathbf{r}) = \int d^3r x^i x^j T^{kl}{}_{|k|l}(\mathbf{r},t) = \frac{\omega^2}{c^2}\int d^3r x^i x^j T^{00}(\mathbf{r}) \qquad (2.102)
$$

This is the quadrupole tensor Q^{ij} of the energy-mass density $\tilde{\rho} = T^{00}/c^2$:

$$
Q^{ij} = \frac{1}{c^2}\int d^3r x^i x^j T^{00}(\mathbf{r}) \qquad (2.103)
$$

Here we consider the non-relativistic case, hence $T^{00} \simeq \rho c^2$. Q^{ij} therefore is the quadrupole tensor of the mass density. Because the deviations of the Minkowskian metric are small, Q^{ij} can be calculated in cartesian coordinates.

We inset 2.100 into 2.97 and therefore obtain

$$
\frac{dP}{d\Omega} = \frac{G\omega^6}{4\pi c^5}\Lambda ij,lmQ^{ij*}Q^{lm} \qquad (2.104)
$$

The dependance on ω^6 is typical for quadrupole radiation. The weak field approximation is justified by the term G/c^5. For the Q^{ij} are constants, the angle dependence is due to the $\Lambda_{ij,kl}$ only, that is to $\hat{\mathbf{k}}$.

We express its components in the cartesic coordinate system by

$$
\left(\hat{k}^i\right) = \left(\hat{k}_x, \hat{k}_y, \hat{k}_z\right) = (\sin\theta\cos\phi, \sin\theta\sin\phi, \cos\theta) \qquad (2.105)
$$

To obtain the total emitted power we must integrate 2.104 with $d\Omega$. With 2.105 we obtain

$$
\begin{aligned}
\int d\Omega \hat{k}_i\hat{k}_j &= \frac{4\pi}{3}\delta_{ij} \qquad (2.106) \\
\int d\Omega \hat{k}_i\hat{k}_j\hat{k}_l\hat{k}_m &= \frac{4\pi}{15}\left(\delta_{ij}\delta_{lm} + \delta_{il}\delta_{jm} + \delta_{im}\delta_{jl}\right) \qquad (2.107)
\end{aligned}
$$

Integration of 2.98 produces

$$
\int d\Omega\Lambda_{ij,kl} = \frac{2\pi}{15}\left(11\delta_{il}\delta_{jm} - 4\delta_{ij}\delta_{lm} + \delta_{im}\delta_{ij}\right) \qquad (2.108)
$$

From 2.104 with 2.106 to 2.108 we obtain

$$
P = \int d\Omega\frac{dP}{d\Omega} = \frac{2G\omega^6}{5c^5}\left(\sum_{i,j}\left|Q^{ij}\right|^2 - \frac{1}{3}\left|\sum_{i} Q^{ii}\right|^2\right) \qquad (2.109)
$$

This is the totally emitted power. As seen above (2.81), the structure of this result can easily be understood. Nevertheless, to obtain the precise expression (dependance on angles, factors) the calculation has to be done.

The large value of $(G/c^5)^{-1} \approx 3.6 \cdot 10^{52} W$ shows that even for high energy densities compared with electromagnetic radiation infalling on earth the effects of deformation of space-time and therefore the effects on h in 2.54 are very small.

Chapter 3

Sources of Gravitational Waves

In this chapter we examine different possible sources of gravitational radiation: Hydrogen, Binary Stars, Pulsars and Supernovaes

3.1 Hydrogen

In the semiclassical image of the Hydrogen an electron (mass m, charge e) surrounds a proton. From the equilibrum of forces $mv^2/a = e^2/a$ and from the quantization of angular momentum $\hbar = mva$ follows the radius $a = \hbar^2/me^2$ and the circular frequency ω_{at}:

$$\epsilon_{at} = \hbar\omega_{at} = \frac{e^2}{a} = mc^2\alpha^2 \tag{3.1}$$

with the finestructure constant $\alpha = e^2/\hbar c \simeq 1/137$. With P_{em} from 2.79 and the dipole moment $p \sim ea$ we estimate the lifetime of an excited state:

$$\tau_{em} \sim \frac{\epsilon_{at}}{P_{em}} \sim \frac{e^2}{a}\frac{c^3}{\omega_{at}^4 e^2 a^2} = \frac{\alpha^{-3}}{\omega_{at}} \sim 10^{-9}\,s \tag{3.2}$$

Similar we estimate the decay of excited states by gravitational radiation. With P_{grav} from 2.81 and with the quadrupole moment $Q \sim ma^2$ we obtain as lifetime

$$\tau_{grav} \sim \frac{\epsilon_{at}}{P_{grav}} \sim \frac{e^2}{a}\frac{c^5}{\omega_{at}^6 Gm^2a^4} \sim \frac{e^2}{Gm^2}\alpha^{-5}\frac{1}{\omega_{at}} \sim 10^{39}10^{10}10^{-15}\,s = 10^{34}\,s \tag{3.3}$$

This rough estimate yields

$$\frac{\tau_{grav}}{\tau_{em}} \sim \frac{1}{\alpha^2}\frac{e^2}{Gm^2} \sim 10^{43} \tag{3.4}$$

what means that on 10^{43} photons there comes only one graviton. Hence the detection by Hydrogen decay itself is hopeless.

3.2 Binary Stars

The two stars in a binary system emit periodical gravitational waves and therefore coalescend. In the case of binary neutron stars the maximal frequency is [4]

$$f_{max} \simeq 1\,kHz \tag{3.5}$$

Currently, three binary neutron star systems are known, in particular the system PSR 1913+16 and very recently the systems PSR 2127+11C and PSR 1534+12 [5].

In the following we calculate the energy flux infalling on earth due to the emission of gravitational waves of a binary system.

A system of binary stars can be treated as rotator. In the rotating coordinate system with coordinates x_i' the quadrupole tensor as defined above (2.103) is

$$\Theta = (\Theta_{ij}) = \left(\int d^3r' x_i' x_j' \rho'(\mathbf{r}')\right) = \begin{pmatrix} I_1 & 0 & 0 \\ 0 & I_2 & 0 \\ 0 & 0 & I_3 \end{pmatrix} \tag{3.6}$$

In an inertial system the coordinates x_i are

$$x_n = (\alpha_n^m(t))\,x_m' \tag{3.7}$$

with the matrix

$$(\alpha_n^m)(t) = \begin{pmatrix} \cos\Omega t & -\sin\Omega t & 0 \\ \sin\Omega t & \cos\Omega t & 0 \\ 0 & 0 & 1 \end{pmatrix} \tag{3.8}$$

and the quadrupole tensor becomes

$$D_{ij}(t) = \left(\alpha(t)\Theta\alpha(t)^T\right)_{ij} \tag{3.9}$$

with the components

$$D_{11}(t) = \frac{I_1+I_2}{2} + \frac{I_1-I_2}{2}\cos(2\Omega t) \tag{3.10}$$

$$D_{12}(t) = \frac{I_1-I_2}{2}\sin(2\Omega t) \tag{3.11}$$

$$D_{22}(t) = \frac{I_1+I_2}{2} - \frac{I_1-I_2}{2}\cos(2\Omega t) \tag{3.12}$$

$$D_{33}(t) = I_3, \quad D_{13}(t) = D_{23}(t) = 0 \tag{3.13}$$

what we can express equally by

$$D_{ij}(t) = c. + [Q_{ij}\exp(-i\omega t) + c.] \tag{3.14}$$

with the frequency

$$\omega = 2\,\Omega \tag{3.15}$$

and the quadrupole moments

$$Q_{11} = Q_{22} = -iQ_{12} = -iQ_{21} \equiv \frac{Ie}{4} \tag{3.16}$$

where we have introduced the inertial moment I and the ellipticity e:

$$I = \frac{I_1 + I_2}{2}, \quad e = \frac{I_1 - I_2}{2} \tag{3.17}$$

Notice that the constant part in 3.14 does not contribute to the emission of waves.

An oscillating quadrupole moment only exists for a rotator not symetrical to the rotational axis, that is for $e \neq 0$. We inset the results in 2.109 and we obtain the totally emitted power:

$$P = \frac{32\,G\Omega^6}{5c^5} e^2 I^2 \tag{3.18}$$

Comparision with 2.81 shows that the relevant quadrupole moment is $\sim eI$. We consider a binary system of two masses M_1 and M_2 at constant distance r as

$$I \simeq I_1 = \frac{M_1 M_2 r^2}{M_1 + M_2}, \quad I_2 \simeq 0, \quad e \simeq 1 \tag{3.19}$$

From the equilibrum of gravitational and centifugal force we obtain the circumference frequency Ω:

$$\frac{M_1 M_2}{M_1 + M_2}\Omega^2 r = G\frac{M_1 M_2}{r^2}, \quad \text{hence} \quad \Omega^2 = G\frac{M_1 + M_2}{r^3} \tag{3.20}$$

Insetting in 3.18 produces the emitted power of the system

$$P = \frac{32}{5}\frac{G^4}{c^5}\frac{M_1^2 M_2^2 (M_1 + M_2)}{r^5} \tag{3.21}$$

This emission significates a loss of energy of the system. Therefore r is decreasing with time.

From observation of the phase-shift of the binary system PSR 1913+16, the circumference time T and the two masses were deduced [6]. Supposing a circular orbit, from 3.20 the distance r is determined.

For the trajectory of PSR 1913+16 is highly elliptical, the calculations become somehow more difficult. A detailed analysis taking in account the propper motion of the system towards the center of the Galaxie leads to a confirmation of better than one percent [7]. This observation actually is regarded as an indirect proof of the existance of gravitational waves.

To examine whether the direct proof of gravitational waves is possible, the energy flux Φ is decisive. We take as example the near binary system i *Boo*. The distance D, the circumference time T and the masses are

$$D = 12pc, \quad T = 0.268d, \quad M_1 = 1.35\ M_\odot, \quad M_2 = 0.68\ M_\odot \tag{3.22}$$

So we have with 3.20 and 3.21 for the totally emitted power

$$P = 3.2 \cdot 10^{23} W \tag{3.23}$$

The energy flux infalling on earth therefore is

$$\Phi = \frac{P}{4\pi D^2} = 1.8 \cdot 10^{-17}\frac{W}{cm^2} \tag{3.24}$$

3.3 Pulsar

The pulsars are systems which emit radiation beams observed as pulses. Because of the high stability of their period, the phase-shift easily can be measured. They are interpreted to be rotating neutron stars.

From the timing observation one can conclude on the electrodynamics of their magnetospheres, on space motions of both single and binary pulsars and on the superfluid interiors of neutron stars. Periods ly within 1.55 ms (PSR 1937+21) up to 4.31 s, mostly between 0.25 s and 1 s [8].

As for the binary stars we want to examine, whether direct proof for gravitational radiation may be possible. As example we take the pulsar NPO 0532 in the center of the crab nebulae at $D \sim 2000pc$. His circumference time is

$$T = \frac{2\pi}{\Omega} = 0.033\ s \tag{3.25}$$

Apart from changes due to star trembling this time is increasing monotonically:

$$\dot{T} = -\frac{2\pi\dot{\Omega}}{\Omega^2} = 4.2 \cdot 10^{-13} \tag{3.26}$$

From the second time derivative in T, the breaking index $\tilde{n} = \tilde{\nu}\nu/\dot{\nu}^2$ can be derived. It allows to decide whether the acceleration is due to magnetic dipole radiation or acceleration of a stellar wind, or whether it is due to gravitational radiation.

The measured values indicate, that magnetic dipole radiation alone does not explain the decrease in frequency [8].

To get an upper limit, we suppose that all energy is emitted by gravitational radiation

$$\frac{d}{dt}E_{rot} = \frac{d}{dt}\left(\frac{I\Omega^2}{2}\right) = I\Omega\dot{\Omega} \equiv -P \overset{3.18}{=} -\frac{32G\Omega^6}{5c^5}e^2 I^2 \tag{3.27}$$

Supposing a mass $M \sim 1.4\ M_\odot$ and a radius $r = 10\,km$ one can estimate the inertia momentum within

$$3 \cdot 10^{44} g\ cm^2 \leq I \leq 3 \cdot 10^{45} g\ cm^2 \tag{3.28}$$

For $I \sim 10^{45} g\ cm^2$ results an ellipticity of

$$e \sim 6 \cdot 10^{-4} \tag{3.29}$$

If the emitted power of the pulsar were due only to gravitational radiation, the energy flux would be greater than for our binary example, namely

$$\Phi = \frac{P}{4\pi D^2} \simeq e^2 \frac{10^{-7} W}{cm^2} \simeq 4 \cdot 10^{-14}\frac{W}{cm^2} \tag{3.30}$$

For the loss due to magnetic dipole radiation is not neglictible, the true value will be less.

3.4 Supernova

A supernova of type II is beliefed to be created by the gravitational collapse of a star to a neutron star state [4].

The basic mechanism consists in the core collapse of a star. This leads to a thermonuclear explosion.

If we suppose a pulse of radiation with

$$\Delta t \sim 0.1s, \quad \Delta\nu \sim 10^3 Hz, \quad \Delta\nu \sim 10^3 Hz \tag{3.31}$$

and an amount of energy ΔE being transformed into gravitational radiation of

$$\Delta E \sim 10^{-6} \ldots 10^{-2} M_\odot c^2 \tag{3.32}$$

we have in the most optimistic case for a supernova in the virgo cluster ($D \simeq 2 \cdot 10^7 pc$) an energy flux during the time Δt of

$$\Phi = \frac{\Delta E}{4\pi D^2 \Delta t} \sim 10^{-6} \frac{W}{cm^2} \tag{3.33}$$

The greatest uncertainty in this calculation comes from the supposition 3.32. Calculations on the collapse are mostly done spherical symmetric [9].

From the Birkhoff-Theorem [1] we know that in a purely spherical collapse no gravitational waves would be emitted.

Calculations on the wave form in the case of non-spherical collapse had been made (see fig. 3.), but there is only poor knowledge in strength and wave forms [4].

As a burst source, the supernova will emit not only at one frequency, but within a bandwith as illustrated in fig. 5c.

3.5 Conclusion on magnitudes

As we will see from eq. 4.1, measuring variations in h can be done with laser provided cavities or delay lines. Two effects lead to a high accuracy:

1. The light can propagate several times (e.g. $n = 50$) between the two mirrors. The optical path length then changes by $n \cdot \delta R$.
2. The precision in measuring the phaseshift $\Delta\Phi$ increases with the number of photons, hence the intensity I_0 of the laser. Therefore $\Delta\Phi \sim \Delta N_\gamma^{-1} \sim N_\gamma^{-1/2}$ holds.

We will examine the measurement techniques more closely in chapter 4. Here we estimate the magnitudes of the effect we must be able to measure.

For two particles in the field of the wave with amplitude h the distance R is changing in the case of long waves ($\lambda \gg R$) corresponding to

$$\frac{\Delta R}{R} \approx h \cos \omega t \tag{3.34}$$

This follows from 2.54 with $\Delta R = R_h - R, e_{11} = h, e_{12} = 0$ and $\phi = \pi/2$.

We will estimate the orders of magnitude for the examples in the preceeding sections. We therefore consider a binary star with the masses $M_1 = M_2 = M$, with the circumference frequency $\Omega = \omega/2$, the distance r between the stars and the distance D to earth. The infalling energy flux is (3.21):

$$\Phi = \frac{P}{4\pi D^2} = \frac{64}{20\pi} \frac{G^4 M^5}{D^2 r^5 c^5} \tag{3.35}$$

[1] A spherical symmetric gravitational field is static.

From 2.76 we have for $e_{11} = h$ and $e_{12} = 0$

$$t_{\mu\nu} = \frac{c^4}{16\pi G} k_\mu k_\nu h^2 \tag{3.36}$$

With $k_0 = k_3 = \omega/c$ results the energy flux of a gravitational wave as function of its amplitude h

$$\Phi = ct_{03} = \frac{c^3 \omega^2}{16\pi G} h^2 \tag{3.37}$$

The frequency Ω of the binary system is given by 3.20. Comparison of 3.35 and 3.37 leads to the dimensionless amplitude of the incident wave:

$$h = \frac{32}{\sqrt{10}} \frac{G^2 M^2}{Drc^4} = \frac{8}{\sqrt{10}} \frac{r_s^2}{Dr} \tag{3.38}$$

with $r_s = 2GM/c^2$.

To put in numbers, we choose

$$M \sim M_\odot, \quad T = \frac{2\pi}{\Omega} \sim 2 \cdot 10^3 s, \quad D \sim 100pc \tag{3.39}$$

With r from 3.20 we obtain

$$h = \frac{\Delta R}{R} \simeq \frac{r_s^2}{Dr} \simeq 10^{-20} \tag{3.40}$$

The same order of magnitude is obtained for the system *i Boo* as can bee seen in fig. 5d.

Our optimistic supposals for the crab pulsar led to an energy flux about 3 magnitudes more than for the binary system. On the other hand, the frequency of the pulsar is higher. For $h^2 \propto \Phi/\Omega^2$ (see 3.37) this in total leads to a decrease in h:

$$h \sim 10^{-23} \tag{3.41}$$

for the crab pulsar.

Making assumptions on the increase in period due to magnetic dipole radiation, the estimated value will be less ($h \sim 10^{-24} \ldots 10^{-26.5}$, see fig. 5d.).

For the supernova we just give a rough estimate. Simplifying by supposing that the emission of the radiation corresponds to an asymmetric collapse with a single frequency Ω_{nova} inferior to that of the pulsar we have due to a flux about 8 magnitudes higher than that of the pulsar

$$h \sim \sqrt{10^8} \frac{\Omega_{pulsar}}{\Omega_{nova}} \gtrsim 10^{-19} \tag{3.42}$$

This is only a very rough estimate. From fig. 5c. follows that supernova events are believed to ly within $h \sim 10^{-17} \ldots 10^{-22}$.

We conclude that systems to measure effects of gravitational waves at least must be able to measure variations in the dimensionless amplitude h of less than 10^{-20}.

It is interesting to ask about the number of gravitational wave sources which will contribute to the overall infall of gravitational radiation. Nakamura et al. [5] give three scenarios of formation of coalescending neutron binaries:

1. The coalescending time of the three known binary neutron stars is $\sim 10^8$ years. Because this time is much smaller than the age of the universe, steady state between the formation rate and the coalescence rate is assumed. The rate of coalescending binary neutron stars is estimated from the rate of supernova II events as 6–60 events $/yr\ (d/100\,Mpc)^3$ within a distance $d\,Mpc$.

2. The second scenario supposes the core of a supernova II to form a thin disk in the collapse. Because such a thin disk is gravitationally instable, it fragments into several pieces. Each fragment will form a neutron star. These neutron stars will coalescend again to form a single neutron star. If the number of fragments is two, the system is a binary neutron star system.

   This scenario increases the event rate within 10 Mpc to ~ 30 events a year.

3. In the third scenario the neutron stars are formed by accretion-induced collapse. For the collapsing white dwarf should have the same angular momentum as the accreting matter, the collapse is supposed to be more or less non-spherical.

Chapter 4

Wave Detection by Interferometrie

In this chapter we will give a brief introduction in the detection of gravitational waves by interferometric devices.

Originally, detetection of gravitational waves was tried to be made by means of resonant absorption in solids, so-called *Weber detectors*. Even if such antennas still exist and physicists spend efforts and hope in them, we will restrict ourselfs on the interferometric devices for the following reasons:

Firstly, prototypes of interferometric detectors have already reached the sensitivity of the best available Weber detectors while possessing a larger spectral bandwith [10]. Secondly, because of the great progress in quantum optics in the last few years one can attend that the precission in controling laser cavities (and therefore to measure phase shifts) will rise enormeously, therefore providing highest potential sensitivity to interferometric detectors. Finally, the greatest projects which are actually faveoured by the governements are all based on interferometrie.

4.1 Principles of Interferometrie

The form of the gravitational waves (fig. 2.) indicates that waves can be measured using the Michelson interferometer as shown in fig. 4a. A gravitational wave with amplitude h of optimal polarization induces length changes δl in each arm of the interferometer according to 2.54:

$$\delta l/l \approx h \cos \omega_g t \tag{4.1}$$

where l is the length of the interferometer arm and ω_g is the frequency of the gravitational wave. For a single lightbeam spending a storage time τ, in the interferometer results a phase change

$$\delta\phi = \int_{-\tau_s}^{0} \frac{4\pi}{\lambda} \delta l dt \tag{4.2}$$

where λ is the wavelength of the utilized light within the interferometer. The signal is at maximum if the storage time τ_s is equal to half the gravitational period since the gravitational wave reverses its sign all half periods.

From the highest frequency of coalescending binaries $f_{max} \simeq 1\,kHz$ (3.5) follows a correspending minimal wavelength $\lambda_{min} \sim 300\,km$. Because the velocities of both particles, that are the gravitons interacting with the photons while passing the interferometer, are c, it follows that the optimal armlength is equal to the minimal wavelength.

To match storage times with reasonable dimensions of the interferometer (armlength of about several km), multipass optical delay lines or Fabry-Perot cavities can be used. As long as any large offset from resonance is assumed to be slow compared with cavity storage times, standard techniques for the analysis of Fabry-Perot interferometers may be used [11].

In a Fabry-Perot cavity, the gravitational wave will interact with the electromagnetic field inside the cavity while inducing sidebands with frequencies

$$\nu \pm \Delta\nu_g$$

, where ν and ν_g are the frequency of the light and the gravitational wave respectively.

For a description of Fabry-Perot techniques, especially the interaction of a laser radiation field with the etalon, we refer to chapter 6.4. in [12]. We briefly resume:

The Fabry-Perot etalon providet by a source of radiation redistributes the radiation into fringes where the wavenumbers corresponding to the different angles are dictated by the etalon spacer, while the spectral profiles of the emitted radiation are defined by the etalon reflectivity. In the case of stimulated emission as a source inside the cavity the interference effect leads to a separation of the modes. Up from an critical population inversion of the involved energy levels coherent emission sets on. This is what is called a laser.

For mode separation, the radiation source does not have to be inside the Fabry-Perot etalon. In the case of a Fabry-Perot resonator provided by a laser, the effect of separation will be amplified for resonant modes. For optimal amplification, the resonator must be tuned to the laser.

Because of the decoupling of the light with storage times of all multiples of $2\ell/c$ the optimal path length cannot strictly be attained. To obtain the path length with optimal storage times delay lines are used. However, since the storage time should rather be regarded as a trade-off between signal and losses for any of the improved techniques (section 4.3) the analysis is to be done seperately.

4.2 Physical Limits

In order to get an idea where effective improvements in the sensitivity of the instruments can be made we consider the actual physical limits. There we have

- photon counting error
- radiation pressure error
- shot noise in the detector
- thermal motion
- seismic noise
- fluctuations of the refractive index
- laser stability

The last mentioned problems are rather technical and therefore must be resolved in their proper domains (photonics, cryotechnics, damping, vacuum technics and feedback circuits). In section 4.3 we will keep the focus on the first two items, which are intrinsic quantum-optical properties of any interferometer.

The figs. 5a. and 5b. show that the technical problems are still dominant in detecting gravitational waves; only for burst sources beating the photon counting limit (indicated as photon noise in the diagramms) would give some improvement.

Here an annotation must be made: Photon noise, as indicated in the diagramms, is sometimes also refered to by shot noise. It must not be changed with the detector shot noise or with fluctuations in the laser-power, for those are not intinsic properties of the interferometer [13]. We refer to photon noise as photon counting error.

The quantum-mechanical uncertainties can be thought to come from three sources: Firstly, they come from the quantum mechanical uncertainties in the end mirrors' position and momenta (refered to as Uncertainty Principle, $m = 400kg$ in the figs. 5a,b.). Secondly, there are pertubations of the end mirrors' positions by radiation pressure fluctuations. Thirdly there is a fluctuation in the number of photons at the output [14] to which we refer to as photon counting error.

In our list we considered the error due to the positions and momenta and the error due to radiation pressure fluctuation as one, to which we refer by radiation pressure error. However, in a rigorous quantitative treatment of all these errors they have to be expressed by an observable quantity, as the corresponding variation in the optical path length $\Delta\ell$ [15]. Nonetheless, the division of the total uncertainty is a useful conceptual device [14].

It can be shown [14] that, as the input laser power P increases, the photon counting error decreases, while the radiation pressure error increases. Real interferometers are currently limited by photon-counting statistics.

By sophisticly preparing the coherent states within the cavities in an interferometer whose performance is not limited by losses in the mirrors, the photon counting error can be reduced while increasing the radiation pressure error. For the Glauber state uncertainty circles [1] in the complexe amplitude plane become squeezed, this technique is referred to as "squeezed-state" technique [14].

The photon counting error according to Poisson statistics is outlined in appendix B.

4.3 Increasing Sensitivity

To improve the intensity of interference fringes against a background noise due to the statistical fluctuations in the number of the detected photons, a variety of techniques have been developed. For they make efficiently use of the light in the interferometer by recyclying, they are referred to as "recycling techniques".

They reduce the photon counting error by increasing the number of photons at the output port of the interferometer.

Multipass optical delay lines or Fabry-Perot cavities are used to match the storage time to the period of the gravitational wave. In the case of slow phase changes compared with the cavity storage time the gain can be calculated from the reflected field. Therefrom the sensitivity and the bandwith of the system can be estimated [11]. We list in the following the different techniques [11]:

standard recycling The simplest version of recycling consists in placing a mirror M_0 in the beam with the correct position to coherently send light back to the cavities or delay lines as shown in figure 4b. The recycling mirror may be regarded as an impendance matching device which ensures efficient resonance. The intensity increases by the effective number of times the light is recycled, thereby enhancing the photon-counting sensitivity by the square root of this factor. An enhancement in sensitivity is obtained for all frequencies – standard recycling produces a broadband detector.

resonant recycling Having a background (e.g. pulsars and accreting neutron stars [4]), narrow band detection will enhance sensivity within a restricted bandwith.

[1] Glauber states can be used to describe a coherent electromagnetic field [16]

In the delay-line case in fig. 4c. the storage time of the light in each arm of the interferometer is arranged to be half a gravitational wave period. The light is then passing into the other arm of the interferometer where, because the gravitational wave changes its sign every half period it sees the same sign of phase shift as it did before. The signal is in resonance with the interferometer and therefore builds up coherently. The signal is increased by the number of times the light is cycled round the whole optical system, which is limited by the losses.

Because the signal instead of the intensity is recycled, the gain is found to be the square of that by using standard recycling. It is restricted to a narrow bandwith since the interferometer must be adjusted resonant to the incomming gravitational wave. Frequencies beside the resonance condition become out of step with the amplified signal and therefore will vanish.

When optical cavities are used for resonant recycling, the detector can be seen as a system of coupled cavities which have two normal modes. The laser resonates with one of these, while the action of the gravitational wave is to pump energy into the other mode. Same as for the delay line system it is not the isolated cavities but the whole system that is on resonance with the incomming wave.

While tuning the detector to higher resonant frequencies, resonant recycling can be made broadband.

tuned recycling This is a technique to make standard recycling narrow band. Within the same optical arrangement as for standard recycling (fig. 4b.) the cavities are tuned so that one of the gravitational wave induced sidebands are on resonance with the isolated cavities. This can be seen as a coupling of the two cavities, leading to a two mode system. The gain and the bandwith are found to be the same as for resonant recycling.

It is possible to choose cavity storage times so that the sensitivy gain is somewhere between the maximum and the broadband value, with a bandwith so that the gain-bandwith product is constant.

dual recycling From the amplitude-phase diagram of the light emerging from a multipass delay line Michelson interferometer can be shown [11] that when the storage time of the delay line is comparable to the gravitational wave period, the phase changes (or sidebands) induced on the light no longer have the correct phase to add most efficiently. Adding the phase shift coherently can be done within resonant recycling techniques, but this can be done even more simple while adding a new recycling mirror M_3 at the output port of the interferometer as shown in fig. 4d.

The mirrors M_0 and M_3 both form optical cavities which enhance the signal. Moreover, they provide an additional degree of freedom: the position of M_3 relative to the image in the beamsplitter of M_0. This allows the phase of the recycled sideband reflected off M_3 and reentering the interferometer arms to be adjusted, so it has exactly the correct phase to add coherently with the sideband being induced by the gravitational wave.

The bandwith of the resonant system for maximized gain is the same as within a cavity resonant recycling system in the case of neglectable losses at M_3. While varying the transmittance of M_3, the bandwith of the system can be varied between the bandwith of the resonant recycling and standard recycling.

This system is not critical to cavity storage time or to phase offset.

4.4 Actual Projects

Prototypes of gravitational wave observatories already exist. Those are the instrument at the MPI Munich, Garching (30 m) [17], at the University Glasglow (10 m), at the Institute for Space and Astronautical Science in Tokyo and an instrument of 40 m at Caltech. They mainly serve to develop new technologies as

- new mirrors
- new optical coatings
- mechanical isolation
- electronic cooling
- losses and noise in semiconductors
- vacuum systems
- feedback circuits
- noise reduction techniques
- data aquisition and analysis

To measure the full information in gravitational waves like direction of the source, time-dependance and polarization a world wide net of detectors is needed. A case study considering up to 5 detectors and the properties of gravitational radiation that can be measured with can be found in [18] The actual projects are [19]

LIGO An USA project consisting in the set-up of two detectors with characteristical legth of 4 km each.

AIGO An australian proposal for a 3 km detector. Not yet confirmed by the governement.

TENKO A japanese 100 m prototype in regard to build a great detector.

VIRGO A french-italian colaboration of a 3 km detector near Pisa.

GEO A german-british colaboration of a 3 km detector near Hannover.

Recently the involved societies CNRS (F), INFN (I) and MPG (RFA) have assigned a common declaration where the SERC (GB) also will adjoin [19]. Currently the european research community is trying to integrate and unify all efforts for the search of gravitational waves.

Appendix A

Electrodynamical Waves

Like Classical Electrodynamics, Einsteins theory of Gravity is also a *Classical Field Theory.* [1] It therefore should not be very astonishing that both theories have elements in common. For we suppose the reader being more familar with Classical Electrodynamics, we give a short recall in this appendix to outline the similarities between the two theories.

Let us start with the inhomogeneous field equation in its covariant form:

$$F^{\alpha\beta}{}_{|\beta} = \frac{4\pi}{c} j^{\alpha} \tag{A.1}$$

with the field tensor $F^{\alpha\beta}$ expressed by the 4 potential fields $A^{\alpha} = (\Phi, A^{i})$:

$$F^{\alpha\beta} = A^{\beta}{}_{|\alpha} - A^{\alpha}{}_{|\beta} \tag{A.2}$$

which automatically satisfies the homogeneous field equations. Equation A.2 holds under the following gauge transformation

$$A^{\alpha} \longrightarrow A^{\alpha} + \partial^{\alpha}\chi \tag{A.3}$$

with an arbitary scalar field χ. This allows to demand an arbitary scalar condition to the potentials. We demand the Lorentz gauge

$$A^{\alpha}{}_{|\alpha} = 0 \tag{A.4}$$

so that the inhomogeneous field equations decouple to

$$\Box A^{\alpha} = \frac{4\pi}{c} j^{\alpha} \tag{A.5}$$

In the case of free fields, that is $j^{\alpha} = 0$ A.4 and A.5 permit another gauge transformation A.3 with a solution χ of the wave equation. This allows another gauge condition $A^{0} = \Phi = 0$. Therefrom the free wave equations can be written

$$\Box A^{\alpha} = 0, \quad A^{0} = \Phi = 0, \quad A^{i}{}_{|i} = 0 \tag{A.6}$$

Therefore only *two independend fields* exist. A complete set of solutions are the plane waves

[1] "Classical" therefore refers to the fact that quantum effects are neglected.

$$\begin{aligned} A^{\alpha} &= e^{\alpha}\exp(-ik_{\beta}x^{\beta}) \quad + c. \\ &= e^{\alpha}\exp(-i\mathbf{kr} - i\omega t) \quad + c. \end{aligned} \tag{A.7}$$

with $(k^{\beta}) = (\omega/c, \mathbf{k})$ and $(x^{\beta}) = (ct, \mathbf{r})$. The equation $\Box A^{\alpha} = 0$ causes

$$k_{\beta}k^{\beta} = 0 \quad \text{or} \quad \omega^2 = c^2k^2 \tag{A.8}$$

with $k = \mid \mathbf{k} \mid$. The amplitude e^{α} of the wave respectively the spatial part e is called polarisation vector. The equations A.8 further restrict this vector according to

$$(e^{\alpha}) = (0, \mathbf{e}), \quad \mathbf{ek} = 0 \tag{A.9}$$

In a coordinate system with x_3 parallel to k the two indepanedant fields are the x_1 and x_2 components:

$$(A^{\alpha}) = (0, e^{1}, e^{2}, 0)\exp(ikx^{3} - i\omega t) + c. \tag{A.10}$$

Therefore two linear polarizations of the wave are possible. They can be indicated by $e^{1} = A$, $e^{2} = 0$ and $e^{1} = 0$, $e^{2} = A$. We obtain circular polarized waves by

$$(A^{\alpha}_{circ}) = A(0, 1, \pm i, 0)\exp(ikx^{3} - i\omega t) \tag{A.11}$$

Rotating the coordinate system by an angle ϕ in x^{3} this solution is transformed according to

$$A^{\alpha}_{circ} \xrightarrow{\text{rotation}} \exp(\mp i\phi)A^{\alpha}_{circ} \tag{A.12}$$

In the quantisized theory A^{α} is the wavefunction of the particles, the photons. Then A.12 means that the photons have spin $\pm\hbar$ in direction of k.

Appendix B

Poisson Statistics

A Poisson distribution is the normalized density distribution in k discrete values

$$p_k = \frac{\lambda^k}{k!}\exp(-\lambda), \quad (k = 0, 1, \ldots) \tag{B.1}$$

with parameter λ.
The first two moments are

$$\begin{aligned} \mu_1 &= \lambda \\ \mu_2 &= \lambda^2 + \lambda \end{aligned} \tag{B.2}$$

Therefore the mean square deviation is

$$\sigma^2 = \mu_2 - \mu_1^2 = \lambda \tag{B.3}$$

In the case of discrete photons being detected at the output port of an interferometer, the expected value of the number of photons N is the first moment, hence

$$\lambda = N \tag{B.4}$$

The relative standard deviation decreases with the number of photons

$$\sigma_{rel} = \sigma/\mu_1 = \frac{1}{\sqrt{N}} \tag{B.5}$$

that is within the intensity of the signal in the interferometer.

Bibliography

[1] P.C.W.Davies, The Search for Gravity Waves, Cambridge UP (1980)

[2] T.Fliessbach, Allgemeine Relativitätstheorie, BI-Wiss.Verl. Mannheim (1990)

[3] S.Weinberg, Gravitation and Cosmology, John Wiley and Sons, New York (1972)

[4] K.S.Thorne, *in* 300 Years of Gravitation, edited by S.W.Hawkings and W.Israel, Cambridge UP, (1987)

[5] T.Nakamura, K.Oohara, *in* The Stucture and Evolution of Neutron Stars, D.Pines (ed.), Addison Wesley (1992) 343

[6] J.M.Weisberg, J.H.Taylor, Phys. Rev. Letter **52** (1984) 1348

[7] T.Damour, J.H.Taylor, Ast. J. **366** (1991) 501

[8] R.N.Manchester, *in* The Stucture and Evolution of Neutron Stars p.32

[9] J.Cooperstein, E.A.Baron, *in* Supernovae, A.G.Petschek (ed.), Springer (1990)

[10] Proposal for a Joint German-British Interferometric Gravitational Wave Detector, MPQ **147**, (1989)

[11] B.J.Meers, Phys. Rev. D **38** (1988) 2317

[12] G.Hernandez, Fabry-Perot Interferometers, Cambridge UP (1986)

[13] C.M.Caves, Phys. Rev. Lett. **45** (1980) 75

[14] C.M.Caves, Phys. Rev. D **23** (1981) 1693

[15] R. Loudon, Phys. Rev. Lett. **147** (1981) 815

[16] R.J.Glauber, Phys. Rev. **131** (1963) 2766

[17] T.M. Niebauer et.al. Phys. Rev. A **43** (1991) 5022

[18] VIRGO-report, Proposal for a Joint French-Italian Interferometric Gravitational Wave Detector, (1989)

[19] K.Denzmann, H.Ruder, Physikalische Blätter **49** (1993) 103

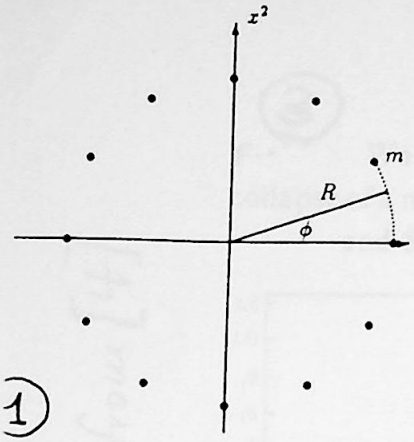

Ring of Particles from [2]

1

from [4]

Two Polarizations of a g.w.

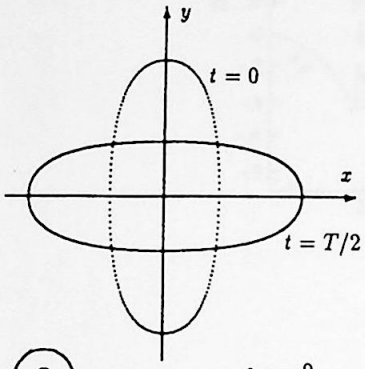

$e_{12} = 0$

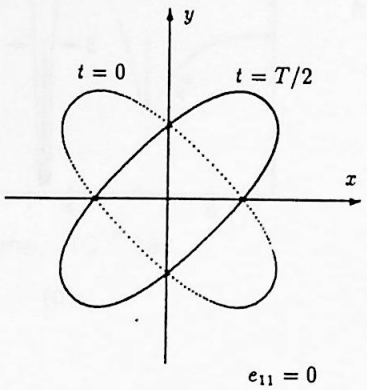

$e_{11} = 0$

2

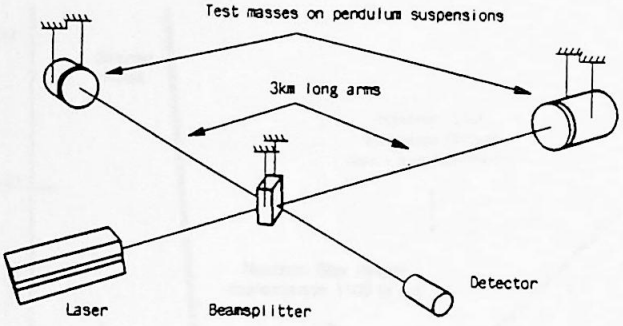

4a from [10]

Diagram illustrating the basic principle of a gravitational wave detector using Michelson interferometry.

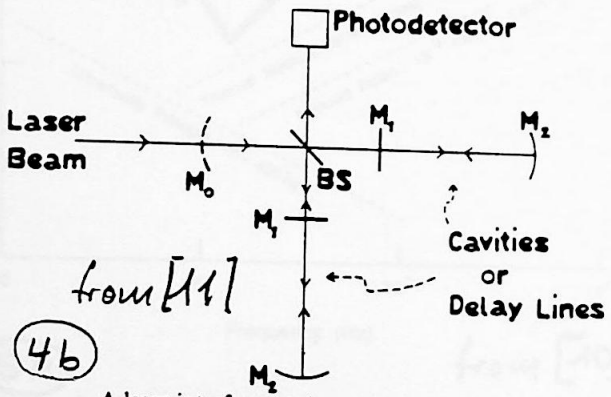

from [11]

4b

A laser-interferometric gravitational-wave detector is essentially a Michelson interferometer. A gravitational wave produces opposite phase shifts on the light in the two arms of the interferometer; when interference occurs at the beamsplitter, the result is an intensity change on the light traveling to the photodetector.

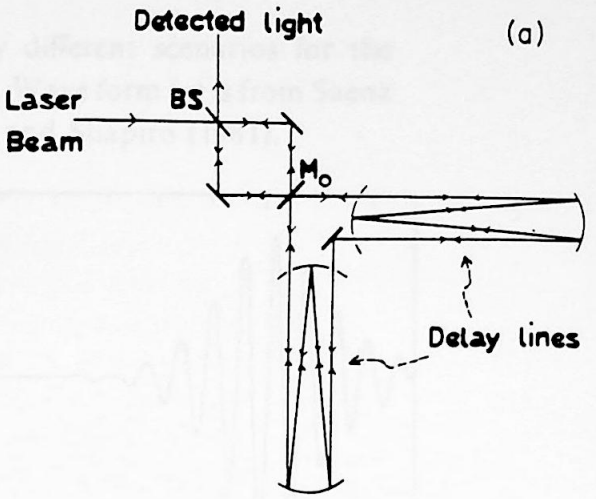

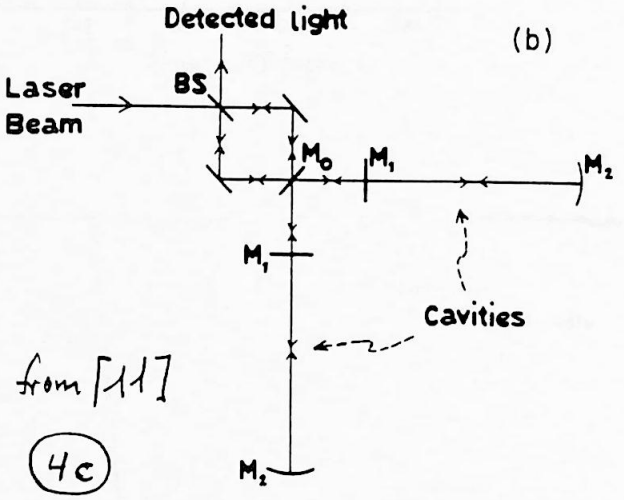

from [11]

4c

A schematic diagram of the optical arrangement for resonant recycling (a) for a delay line, (b) for a cavity.

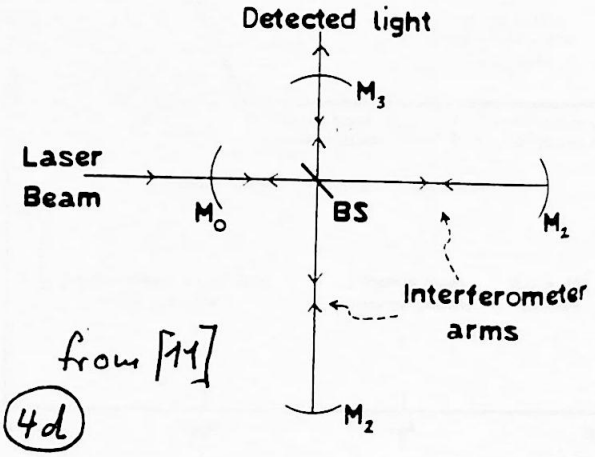

from [11]

4d

The proposed new arrangement for recycling ("dual recycling"): the new element is the mirror M_3 which ensures that both signal and intensity are recycled. The optical elements in the arms of the interferometer can be either single or multipass delay lines or cavities. Viewed from M_3, the interferometer must operate on a dark fringe if differential motion of the two arms is to be enhanced.

(3)

F[illegible] Wave forms produced by two very different scenarios for the collapse of a normal star to form a neutron star. Wave form (*a*) is from Saenz and Shapiro (1978); (*b*) is from Saenz and Shapiro (1981).

from [4]

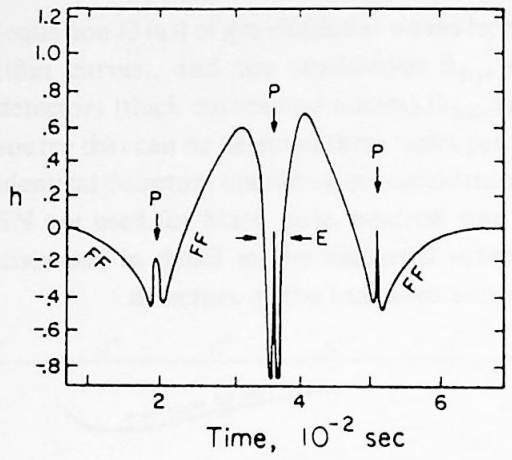

(a)

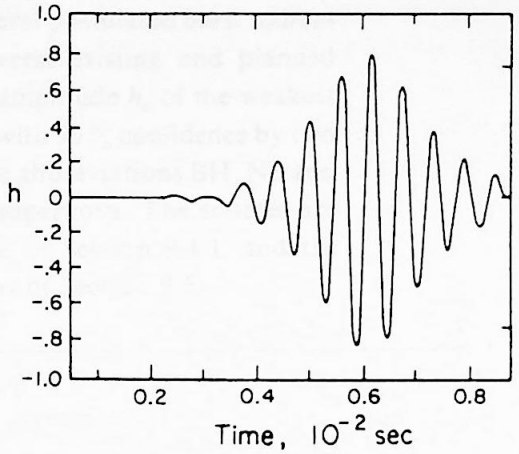

(b)

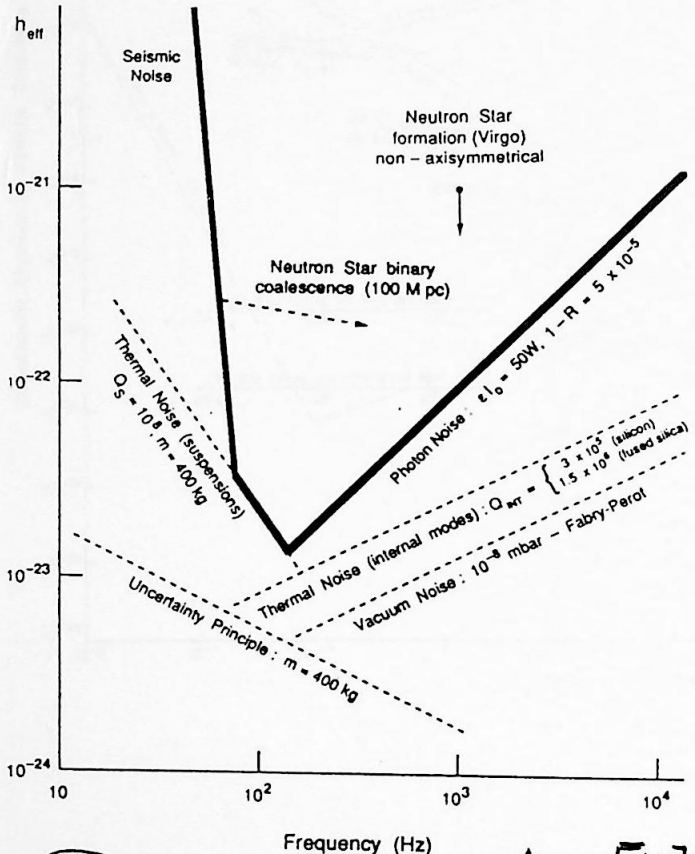

(5a)

from [10]

Some burst sources and relevant noise levels. The ordinate is the effective amplitude h_{eff}, which is defined as $(S/N)\sigma_{bb}(f)$, where S/N is the signal-to-noise ratio given for different sources in the text and $\sigma_{bb}(f)$ is the value of the photon noise at the burst's central frequency f, as shown in the figure. For sources that have to be picked out by filtering, the effective amplitude is approximately $h\sqrt{n/2}$, where h is the true amplitude and n is the number of cycles of the waveform over which the signal can be integrated.

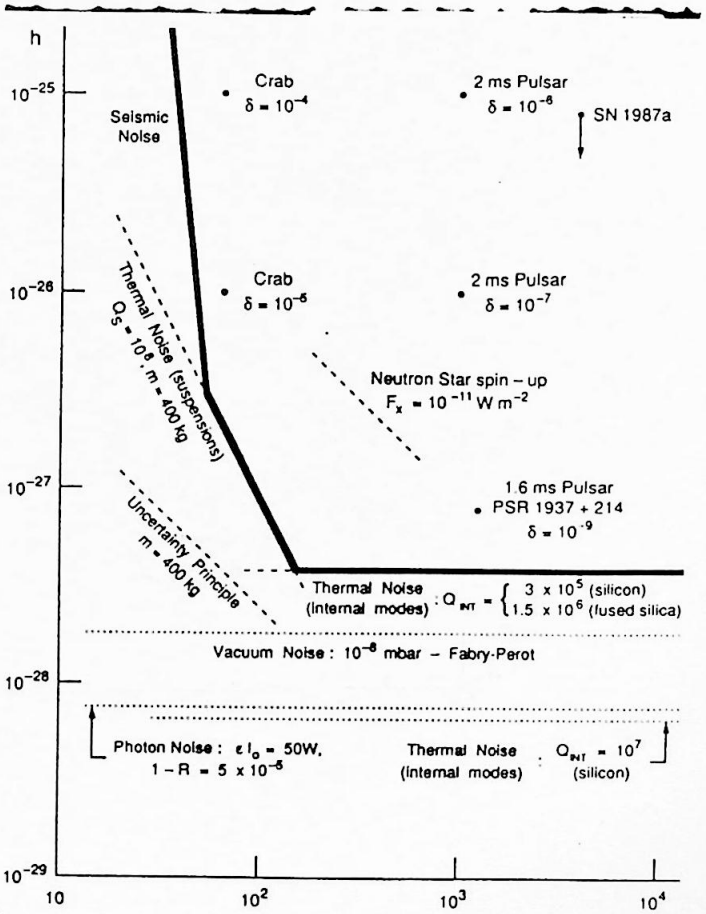

(5b)

from [10]

Signals from possible sources of continuous radiation. An integration time 10^7 s is assumed. Note that due to possible non-optimum relative orientatio of source and detector, signal strengths may need to be reduced by a facto of up to $\sqrt{5}$. Thermal noise for Q_{INT} ranging from 3×10^5 to 10^7 is shown representing estimated lower and upper limits to the internal Q of suspende

(5c)

from [4]

The characteristic amplitudes h_c (equation (31b)) and frequencies f_c (equation (31a)) of gravitational waves from several postulated *burst sources* (thin curves), and the sensitivities $h_{3/yr}$ of several existing and planned detectors (thick curves and circles) ($h_{3/yr}$ is the amplitude h_c of the weakest source that can be detected three times per year with 90% confidence by two identical detectors operating in coincidence). The abbreviations BH, NS and SN are used for black hole, neutron star and supernova. The sources are discussed in detail in the indicated subsections of Section 9.4.1, and the detectors in the indicated subsections of Section 9.5.

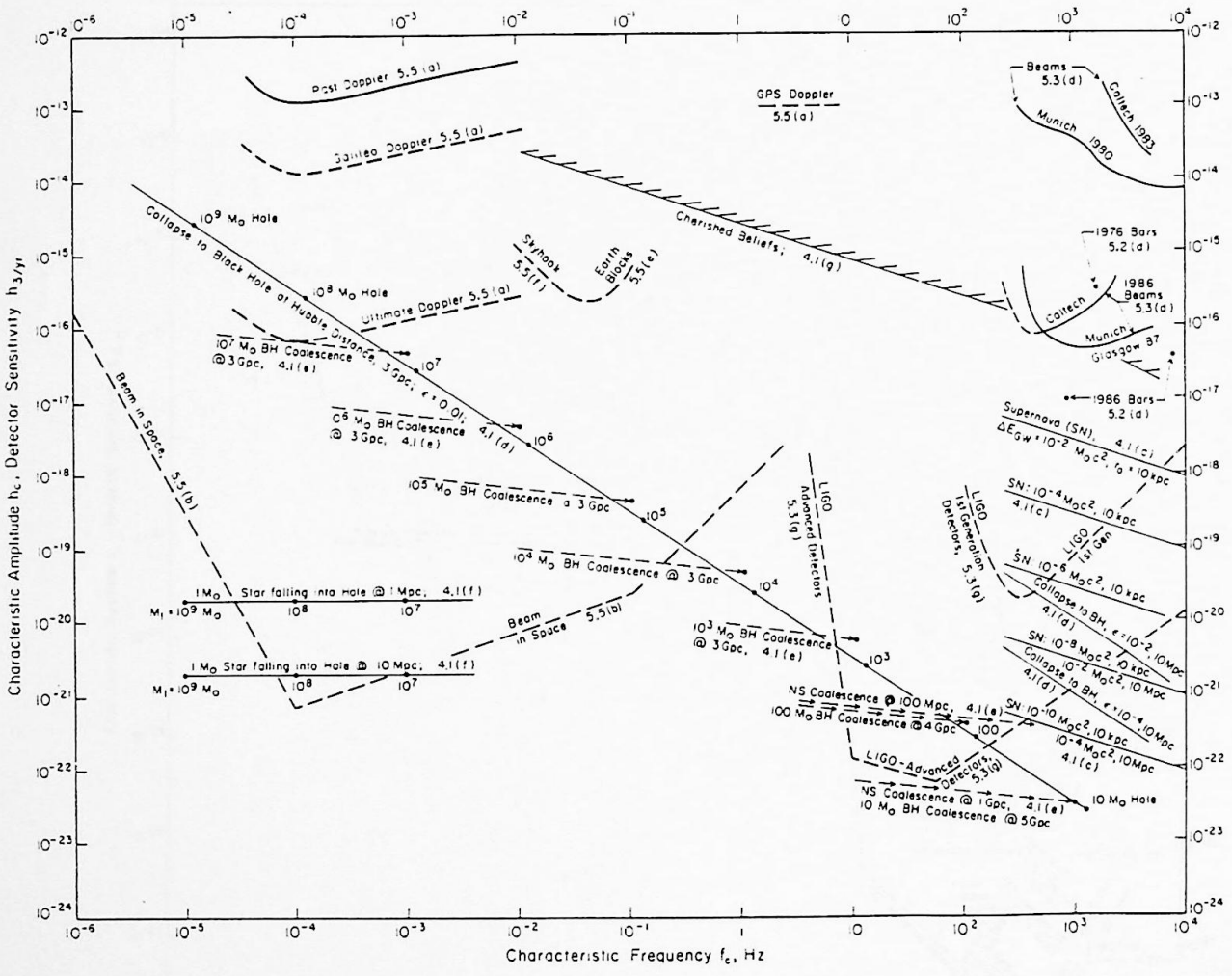

5d

from [47]

The characteristic amplitudes h_c (equation (50)) and frequencies f of waves from several postulated *periodic sources* (thin curves), and the sensitivities $h_{3/\mathrm{yr}}$ of several existing and planned detectors (thick curves and circles) ($h_{3/\mathrm{yr}}$ is the amplitude h_c of the weakest source detectable with 90% confidence in a $\frac{1}{3}$ yr $= 10^7$ s integration if the frequency and phase of the source are known in advance; equation (52a)). The sources shown in the high-frequency region, $f \gtrsim 10$ Hz, are all special cases of rotating, nonaxisymmetric neutron stars (Section 9.4.2(b)). The steeply sloping dotted lines labeled NS Rotation refer to rigidly rotating neutron stars with moment of inertial $I_{zz} = 10^{45}$ g cm^{-2}, and with various ellipticities ε and distances r labeled on the lines (equation (55)). The sources in the low-frequency region, $f \lesssim 0.1$ Hz, are all binary star systems in our galaxy (Section 9.4.2(c)): several specific, known binaries, which are indicated by name (μ Sco, V Pup, ...); the strongest six spectral lines from the famous binary pulsar PSR1913 + 16; and the estimated strengths of the strongest white-dward ('WD') and neutron-star ('NS') binaries in our galaxy. The detectors are discussed in detail in the indicated subsections of Section 9.5.